Teleportation using squeezed single photons

Agata M. Brańczyk and T. C. Ralph

Center for Quantum Computer Technology, Department of Physics, The University of Queensland, QLD 4072, Australia

(Received 25 June 2008; published 4 November 2008)

We present an analysis of squeezed single photon states as a resource for teleportation of coherent state qubits and propose proof-of-principle experiments for the demonstration of coherent state teleportation and entanglement swapping. We include an analysis of the squeezed vacuum as a simpler approximation to small-amplitude cat states. We also investigate the effects of imperfect sources and inefficient detection on the proposed experiments.

I. INTRODUCTION

Coherent state quantum computing (CSQC) [1,2] is an optical approach to quantum computing which relies solely on linear optics, state preparation, and measurement, rather than in-line optical nonlinearities. Unlike in single photon linear optical quantum computing (LOQC) [3,4]—where qubits are encoded in the polarization, path, frequency, etc. of single photons—in CSQC, qubits are encoded in the phase and amplitude of coherent states. The qubit basis is defined as $|0\rangle = |\alpha\rangle$ and $|1\rangle = |-\alpha\rangle$. The basis is only approximately orthogonal where $\langle \alpha | -\alpha \rangle = e^{-2|\alpha|^2}$, however, for $|\alpha| > 2$, the overlap is practically zero ($< 4 \times 10^{-4}$).

In both CSQC and LOQC, teleportation is used to implement gates [5]. A key practical difference between the two schemes is that a simple teleportation scheme, with a high probability of success, exists for CSQC [6,7], whilst simple LOQC teleportation only works with a 50% success rate [8]. More generally, in the Knill-Laflamme-Milburn scheme the probability of teleportation scales as $n/(n+1)$, where n is the number of photons in the entangled state used as a resource and the complexity of the circuit increases with n [3]. This leads to a significant saving in the overheads for computation.

It was thought that $\alpha \geq 2$ was needed in order to implement the required gates for quantum computing, due to the nonorthogonality of coherent state qubits [9]. More recently, however, Lund *et al.* [2] presented a universal set of gates for quantum computing which work even for small α. In this scheme, the size of the coherent state has no effect on the fidelity of the gate—only on the probability of success of the gate. Indeed, below a certain α, these gates could not be used for scalable quantum computing, as the probability of success would be too low, nevertheless the probability of success can still be significantly greater than the LOQC bound of 50%. Such heralded gates open the door to a range of exciting possibilities for proof-of-principle experimental implementation of coherent state quantum computing.

The difficulty in performing these (and previous) gates does not arise from our inability to create large-amplitude coherent states—these are very well approximated by the output of a laser. The difficulty arises from our inability to create *superpositions* of coherent states with large α. Such coherent state superpositions, known in the literature as *cat states*, have not yet been experimentally realized.

However, small-amplitude cat states can be approximated—in some cases, very well—using photon-subtracted squeezed vacuum states [10]. Such states have already been experimentally demonstrated [11,12]. We note that a photon-subtracted squeezed vacuum state is mathematically equivalent to a squeezed single photon state. These terms will be used interchangeably depending on context throughout this paper. In this paper, we will also examine the squeezed vacuum state as a less complicated way of generating cat state approximations. We will not discuss approximations to small-amplitude cat states via homodyne postselection [13].

This paper is organized as follows. In Sec. II we revisit the coherent state teleportation protocol introduced in [6,7]. In Sec. III we discuss approximations to cat states, in particular, the squeezed single photon state. We then analyze how well these squeezed single photon states perform as resource states for the teleportation of arbitrary coherent state qubits in Sec. IV. In Sec. V, we propose experimentally realizable demonstrations of coherent state teleportation using squeezed single photons. In Sec. VI, we analyze the effect of imperfect state preparation and inefficient detection on the teleportation scheme before we conclude and discuss our results in Sec. VII.

II. TELEPORTATION

The gates presented in [2] are all variations of the quantum teleportation scheme [6,7,14] shown in Fig. 1. We will use this teleportation scheme as the basis for our proof-of-principle experiments. Refer to the caption in Fig. 1 for a brief review of teleportation using cat-states.

A cat state is an equal coherent superposition of two coherent states $|\beta\rangle$ and $|-\beta\rangle$, where

$$|\beta\rangle = e^{-|\beta|^2/2} \sum_{n=0}^{\infty} \frac{\beta^n}{\sqrt{n!}} |n\rangle. \tag{1}$$

Using an odd cat $|\beta\rangle_b - |-\beta\rangle_b$ as the resource state, the combined input state can be written as follows (ignoring normalizations):

$$|\psi_{\text{in}}\rangle_{a,b,c} = (\mu|\alpha\rangle_a + \nu|-\alpha\rangle_a)(|\beta\rangle_b - |-\beta\rangle_b)|0\rangle_c. \tag{2}$$

In this paper, we will use the convention that α refers to the initial amplitude of the input states in mode a and β refers to
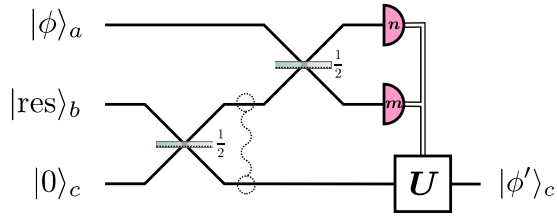
FIG. 1. (Color online) Teleportation scheme for teleporting the state $|\phi\rangle_a = \mu|\alpha\rangle_a + \nu|-\alpha\rangle_a$. A resource state, $|\text{res}\rangle_b = |\beta\rangle_b \pm |-\alpha\rangle_b$, incident on a 50:50 beam splitter, creates a coherent-state Bell pair in modes b and c. After the second beam splitter, photon-number measurements of modes a and b project the state in mode c into $|\phi'\rangle_c = |\phi\rangle_a$ (up to local unitaries). Depending on the measurement results, the remaining qubit may need to be corrected. The corrections (for an odd cat resource state) are as follows: n=odd, m=0, $U \to I$; n=0, m=odd, $U \to X$; n=even, m=0, $U \to Z$; n=0, m=even, $U \to XZ$, where X and Z are Pauli operators and I is the identity operation. For experimental realisation of this scheme, $|\text{res}\rangle_b = \hat{S}_r|1\rangle_b$ and $|\phi\rangle_a = |\alpha\rangle_a$, $\hat{S}_{r'}|1\rangle_a$ or $\hat{S}_{r''}|0\rangle_a$, where $r = r_{\text{opt}}(\beta)$, $r' = r_{\text{opt}}(\alpha)$, $r'' = r_{\text{opt-v}}(\alpha)$ and $\beta = \sqrt{2}\alpha$. The squiggly line emphasizes entanglement between qubits.

the initial amplitude of the resource states in mode b and $\beta = \sqrt{2}\alpha$. The first beam splitter turns the resource state in mode b into a coherent-state Bell pair in modes b and c:

$$|\psi_{\text{BS}}\rangle_{a,b,c} = (\mu|\alpha\rangle_a + \nu|-\alpha\rangle_a)(|\alpha\rangle_b|\alpha\rangle_c - |-\alpha\rangle_b|-\alpha\rangle_c). \tag{3}$$

Just before the photon number measurement, the three-mode state is

$$\begin{aligned}|\psi\rangle_{a,b,c} = &\mu|\beta,0,\alpha\rangle_{a,b,c} - \mu|0,\beta,-\alpha\rangle_{a,b,c} \\ &+ \nu|0,-\beta,\alpha\rangle_{a,b,c} - \nu|-\beta,0,-\alpha\rangle_{a,b,c}.\end{aligned} \tag{4}$$

From Eq. (4), it can be seen that photon-number measurements of modes a and b will project the state in mode c into $\mu|\alpha\rangle_c + \nu|-\alpha\rangle_c$, or some known variation which can be corrected with single qubit Pauli operations (see Fig. 1). In practice, only the X correction (which is simply implemented using a phase shifter) needs to be performed for gate applications [15]. Here we assume corrections are done after detection of the output state. This is called working in the "Pauli frame" [16].

Ideally, it is not possible to detect a nonzero number of photons in both detectors simultaneously. The teleportation fails when both detectors get the result 0. As α increases, the probability of there being a $|0\rangle$ component in a coherent state decreases, therefore the probability of getting the result $m = n = 0$ also decreases, resulting in an increased probability of success. This happens at different rates depending on the input state. In the unique case of the input state being an odd cat state, there are never any $m = n = 0$ components and therefore the success probability is always 1. The solid curves in Fig. 2 show the success probabilities for a selection of input states which range between two extremities. When the gate succeeds, it does so with unity fidelity.
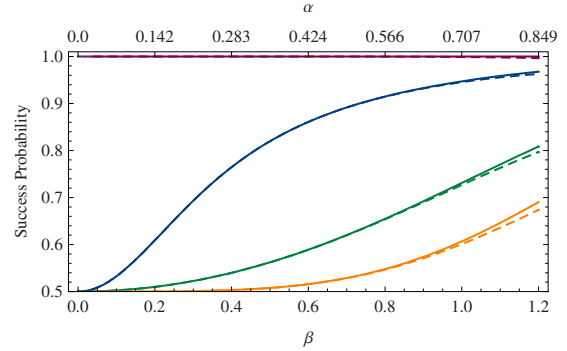

FIG. 2. (Color online) Success probabilities of the teleportation scheme shown in Fig. 1 using $|\text{res}\rangle = |\beta\rangle - |-\beta\rangle$ (solid) and $|\text{res}\rangle = \hat{S}_r|1\rangle$ (dashed). The input states are (from top to bottom) $\frac{1}{\sqrt{2}}|\alpha\rangle - \frac{1}{\sqrt{2}}|\alpha\rangle$ (red), $\frac{1}{2}|\alpha\rangle - \frac{\sqrt{3}}{2}|\alpha\rangle$ (blue), $|\alpha\rangle$ or $|-\alpha\rangle$ (green), and $\frac{1}{\sqrt{2}}|\alpha\rangle + \frac{1}{\sqrt{2}}|\alpha\rangle$ (yellow). Notice that the success probability is always larger than that of the LOQC scheme which cannot succeed more than half of the time.

III. APPROXIMATING CAT STATES

In this section, we will discuss experimentally realizable approximations to cat states. We will use the fidelity $F(\rho, |\phi\rangle) = \langle\phi|\rho|\phi\rangle$ as a measure of how alike two states are, and therefore as a measure of how well these states approximate cat states. The fidelity ranges between 0, where the states are orthogonal, and 1, where the states are equal.

Consider even and odd cat states of amplitude β [17] as follows:

$$|\text{even cat}\rangle = N_+(|\beta\rangle + |-\beta\rangle) = N_+ e^{-|\beta|^2/2}\sum_{n=0}^{\infty}\frac{2\beta^{2n}}{\sqrt{2n!}}|2n\rangle, \tag{5}$$

$$\begin{aligned}|\text{odd cat}\rangle &= N_-(|\beta\rangle - |-\beta\rangle) \\ &= N_- e^{-|\beta|^2/2}\sum_{n=0}^{\infty}\frac{2\beta^{2n+1}}{\sqrt{(2n+1)!}}|2n+1\rangle,\end{aligned} \tag{6}$$

where $N_\pm = 1/\sqrt{2(1 \pm e^{-2|\beta|^2})}$. By writing the cat states in the Fock basis, we see that the even (odd) cat state contains only even (odd) photon number terms.

The squeezed vacuum state

$$\hat{S}_r|0\rangle = \sum_{n=0}^{\infty}\frac{(\tanh r)^n}{\sqrt{\cosh r}}\frac{\sqrt{2n!}}{2^n n!}|2n\rangle, \tag{7}$$

where r is the squeezing parameter, also contains only even photon number terms. The squeezed single photon is a Gaussian state, but nevertheless it is a high-fidelity ($F > 0.99$) approximation to the small-amplitude ($\beta \lesssim 0.75$) even cat state. Optimizing over r, we find that the fidelity between $|\beta\rangle + |-\beta\rangle$ and $\hat{S}_r|0\rangle$ is at a maximum when $r_{\text{opt-v}}(\beta) = \ln(\sqrt{2\beta^2 + \sqrt{1+4\beta^4}})$. Figure 3(a) shows how this fidelity and the optimum amount of squeezing r vary as a function of β. If one photon is subtracted from the squeezed vacuum state, the resulting state contains only odd photon-number terms and is a high-fidelity ($F > 0.99$) approximation
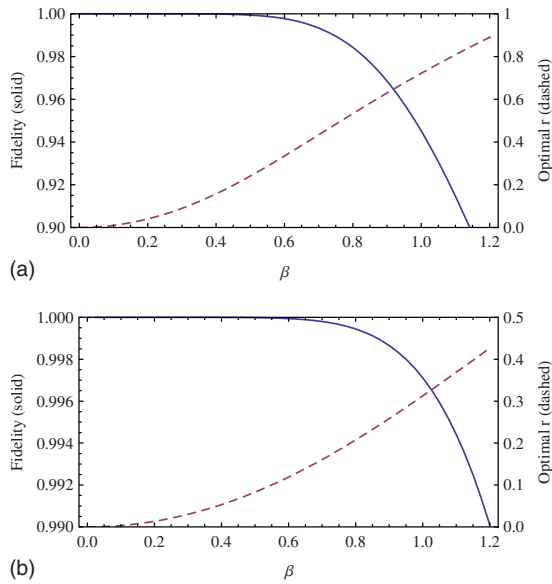
FIG. 3. (Color online) (a) The fidelity between an even cat state and a squeezed vacuum state (solid) and the optimal squeezing parameter, r (dashed), as a function of α. (b) The fidelity between an odd cat state and a squeezed single photon (solid) and the optimal squeezing parameter, r (dashed), as a function of α. Notice different scales for the fidelities and the optimum squeezing parameters between (a) and (b).

to the small-amplitude ($\beta \lesssim 1.2$) odd cat state [18]. We remind the reader that this is also the squeezed single photon state:

$$\hat{a}\hat{S}_r|0\rangle = \hat{S}_r|1\rangle = \sum_{n=0}^{\infty} \frac{(\tanh r)^n}{(\cosh r)^{3/2}} \frac{\sqrt{(2n+1)!}}{2^n n!} |2n+1\rangle. \quad (8)$$

Figure 4 shows the Wigner functions for odd cat states of amplitudes $\beta=2$ and $\beta=1$, as well as for a squeezed single photon. Optimizing over r, we find that the fidelity between $|\beta\rangle - |-\beta\rangle$ and $\hat{S}_r|1\rangle$ is at a maximum when $r_{\rm opt}(\beta) = \ln(\sqrt{\frac{2\beta^2}{3} + \frac{1}{3}\sqrt{9+4\beta^4}})$.

Figure 3(b) shows how this fidelity and the optimum amount of squeezing r vary as a function of β. One can continue to subtract more photons, each time creating a better approximation to either an even or an odd cat state, however, this very quickly becomes extraordinarily challenging to implement experimentally. A theoretical analysis of this method was performed in Refs. [18,19].

In this paper, we focus on the squeezed single photon, as it is a better cat-state approximation than the squeezed vacuum state, and has already been experimentally demonstrated [11,12]. However, we will include results for the squeezed vacuum state for comparison and to see just how well one can do with a Gaussian state. In the next section, we will investigate the eligibility of the squeezed single photon state as an approximation to an odd cat state, for the purposes of proof-of-principle implementation of the quantum teleportation described in [2].

We emphasize that it should not be taken for granted that a high-fidelity approximation to a cat state will necessarily
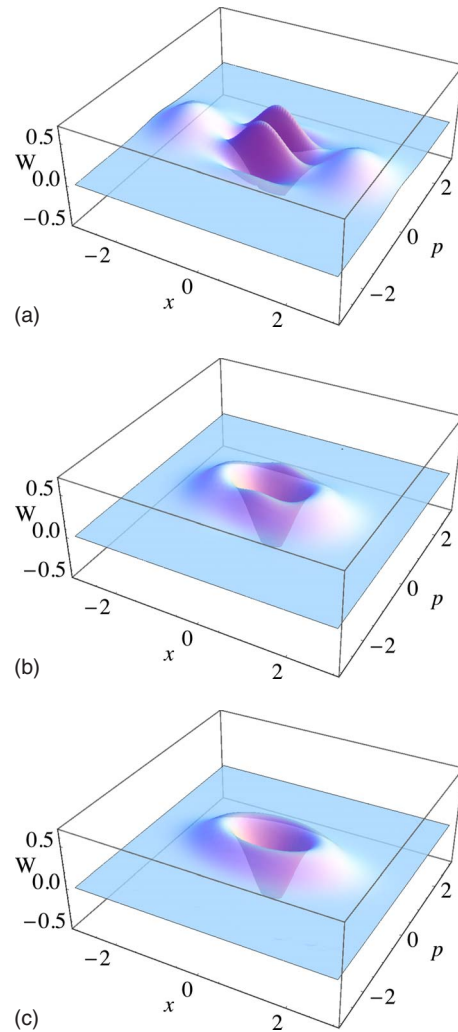

FIG. 4. (Color online) The Wigner function W, where x and p are the in-phase and out-of-phase quadratures, respectively, for an odd cat state $|\beta\rangle - |\beta\rangle$ where $\beta=2$ (a), an odd cat state where $\beta=1$ (b), and a squeezed single photon $\hat{S}_r|1\rangle$ where $r=r_{\rm opt}(1) \approx 0.31$ (c). Notice that at $\beta=1$, the Wigner functions for the cat state looks very much like for the squeezed single photon. This becomes more pronounced at even lower β. In the limit of $\beta \to 0$, the odd cat state becomes an unsqueezed single photon.

perform well in CSQC protocols. Take the example of the cat breeding protocol introduced by Lund *et al.* and Jeong *et al.* [10,20]. Using this scheme, it is possible to create larger cat states by interferring two smaller cat states on a beam splitter, then performing a measurement on one of the output modes. When a squeezed vacuum state is used as an approximation to an even cat state in this protocol, the resultant state is not the expected approximation to a larger cat state, but rather the same sized squeezed vacuum state that was input into the scheme. This is in spite of the high fidelity between the squeezed vacuum and the even cat state at small α.

IV. SQUEEZED SINGLE PHOTON AS A RESOURCE

In this section, we will examine how well coherent state (CS) teleportation can be implemented using a squeezed
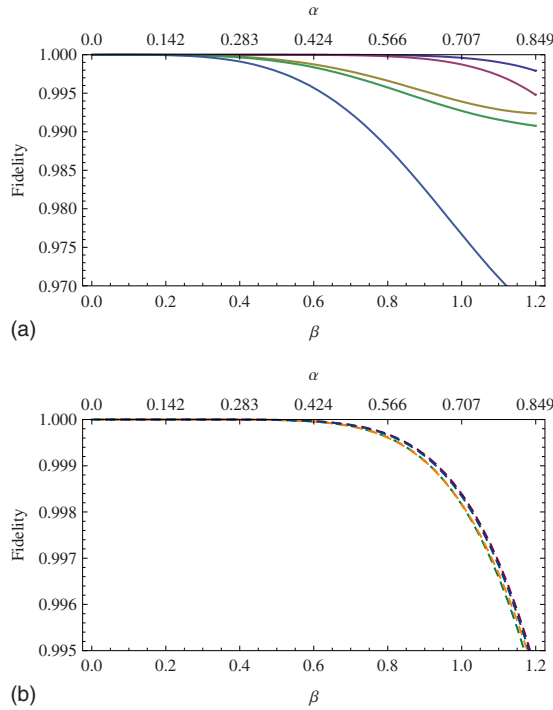
FIG. 5. (Color online) (a) Fidelities for the teleportation of $|\phi\rangle_a = |\alpha\rangle - |-\alpha\rangle$ using $|res\rangle_b = \hat{S}_r|1\rangle$ given different photon-number measurement results (from top to bottom) $m = 1, 2, 3, 4,$ and 5. (b) Fidelities for the teleportation scheme using $|res\rangle_b = \hat{S}_r|1\rangle$ and a variety of input states (from top to bottom): $|\alpha\rangle - |\alpha\rangle$ (red); $\frac{1}{2}|\alpha\rangle + \frac{\sqrt{3}}{2}|\alpha\rangle$ (blue); $|\alpha\rangle + |\alpha\rangle$ (yellow); and $|\alpha\rangle$ or $|-\alpha\rangle$ (green). The input state has only a minor effect on the fidelity.

single photon as a resource. In Sec. III, we showed that the squeezed single photon is a very good approximation to a small-amplitude odd cat state (and that the squeezed vacuum is also a good approximation to an even cat state, but at smaller amplitudes).

To characterize how well the $\hat{S}_r|1\rangle$ theoretically performs as a resource for teleportation, we will calculate the fidelity $F(|\phi\rangle_a, |\phi'\rangle_c)$ between the input state $|\phi\rangle_a$ and the output state $|\phi'\rangle_c$. Since our resource state is only approximate, we will not have perfect interference at the beam splitters. This will have three consequences. The first will be variations in the output state depending on the photon-number measurement results, as demonstrated in Fig. 5(a). By taking into account the different possible output states and the probability with which we expect for them to occur, we can calculate the *average* fidelity. One reason for this variation in fidelities, given different photon-number measurement results, is due to r being optimized to maximize the fidelity between $|res\rangle_b = \hat{S}_r|1\rangle$ and $|res\rangle_b = |\beta\rangle - |-\beta\rangle$. This will maximize the average fidelity for the teleporter, but not the individual fidelities for each different photon-number result. The second consequence of the imperfect interference will result in an input-state-dependent fidelity as demonstrated in Fig. 5(b). This is only a small effect. Notice that the fidelity drops as a function of α. This is solely due to the inadequacy of the $\hat{S}_r|1\rangle$ as an approximation to an odd cat state at high amplitudes, and not an artifact of the gate itself.

The third consequence of the imperfect interference will be an additional way in which the gate can fail. Not only will it fail if we measure zero photons in both detectors, it will also fail if we measure a nonzero number of photons in both detectors *simultaneously*, something which was not possible when we had perfect interference. This will result in a slightly decreased probability of success, which begins to manifest itself at larger amplitudes whereas the $m = n = 0$ events are only problematic at low amplitudes. This is shown by the dashed curves in Fig. 2.

One might expect that the the squeezed single photon will only be as good a resource as it is an approximation to an odd cat state. It is interesting to note that it is actually better. A squeezed single photon $\hat{S}_r|1\rangle$ will have a certain fidelity when compared with an odd cat state $|\beta\rangle - |-\beta\rangle$, however, using that resource for teleporting $|\phi\rangle_a = |\alpha\rangle - |-\alpha\rangle$ results in teleportation with a higher fidelity for a given β.

In the next section, we will look at teleporting physically realizable input states.

V. PROPOSED EXPERIMENTS

In the previous section, we demonstrated that a squeezed single photon could be, in theory, a resource for teleportation of arbitrary superpositions of small-amplitude coherent states, however, at present, we are unable to create such superpositions. In this section we propose two types of experiment. The first is the teleportation of three particular example states: a squeezed single photon as an approximation to an odd cat state, a squeezed vacuum as an approximation to an even cat state, and a coherent state. The second is an entanglement swapping scheme which demonstrates the effective teleportation of an arbitrary superposition of coherent states. In our calculations, the photon-number expansion of the states in this section were truncated at $n = 15$, which was sufficient for accurate results up to $\beta = 1.2$.

A. Teleportation

We will demonstrate CS teleportation by using the resource state $|res\rangle = \hat{S}_r|1\rangle$ to teleport the following input states: a squeezed single photon $\hat{S}_{r'}|1\rangle$ as an approximation to an odd cat state $|\alpha\rangle - |-\alpha\rangle$; a squeezed vacuum state $\hat{S}_{r'}|0\rangle$ as an approximation to an even cat state $|\alpha\rangle + |-\alpha\rangle$; and a coherent state $|\alpha\rangle$.

To teleport a squeezed single photon $\hat{S}_{r'}|1\rangle$ using another squeezed single photon $\hat{S}_r|1\rangle$, we need to match the optimal squeezing parameters r and r'. This can be achieved by relating the squeezed single photons to the odd cat states they are intended to approximate. This gives $r = r_{opt}(\beta)$ and $r' = r_{opt}(\alpha)$, where $\beta = \sqrt{2}\alpha$. We have calculated the fidelity averaged over only the odd photon-number results. For even results, a Z correction is required, which would involve sending the output state through another gate making a meaningful comparison between the input and output states of the teleporter difficult. Allowing for the X correction is easy as it simply corresponds to a π phase shift. All further fidelities shown in this section have also been averaged over odd
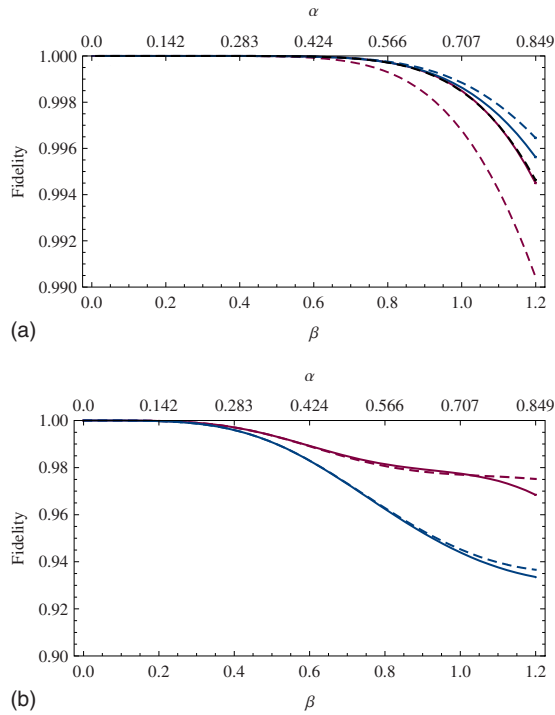
FIG. 6. (Color online) (a) Fidelities for teleportation using $|res\rangle_b = \hat{S}|1\rangle_r$ and teleporting (solid, from top to bottom): $|\phi\rangle_a = |\alpha\rangle - |-\alpha\rangle$ and $|\phi\rangle_a = |\alpha\rangle + |-\alpha\rangle$ as well as (dashed, from top to bottom) $|\phi\rangle_a = \hat{S}_{r'}|1\rangle_a$, $|\phi\rangle_a = |\alpha\rangle_a$, and $|\phi\rangle_a = \hat{S}_{r'}|0\rangle_a$. (b) Fidelities for teleportation using $|res\rangle_b = \hat{S}_r|0\rangle_a$ and teleporting (solid, from top to bottom): $|\phi\rangle_a = |\alpha\rangle + |-\alpha\rangle$ and $|\phi\rangle_a = |\alpha\rangle - |-\alpha\rangle$ as well as (dashed, from top to bottom) $|\phi\rangle_a = \hat{S}_{r''}|0\rangle_a$, and $|\phi\rangle_a = \hat{S}_{r'}|1\rangle_a$. Notice different scales for the fidelity.

photon-number results, for consistency. We also calculated the fidelity for teleporting $|\phi\rangle_a = |\alpha\rangle_a - |-\alpha\rangle_a$ using $|res\rangle_b = \hat{S}_r|1\rangle_b$. Both results are shown in Fig. 6(a). For easy comparison with other figures, we have plotted the fidelity as a function of the effective β for the squeezed single photon, rather than the squeezing parameter r.

To teleport the squeezed vacuum state, we set $r'' = r_{\text{opt-v}}(\alpha)$. The fidelities for teleporting $\hat{S}_{r'}|0\rangle$ and $|\alpha\rangle + |-\alpha\rangle$ are also shown in Fig. 6(a), as is the fidelity for teleporting $|\phi\rangle = |\alpha\rangle$. While there is some variation in the fidelity for the different input states, in the region where $\beta \lesssim 1.2$, the fidelity is always >0.99, even when we teleport the squeezed vacuum state.

Using the squeezed vacuum state as a resource for teleportation, however, does not do as well. This is because the resource state needs to be higher in amplitude than the input state and the squeezed vacuum is not as good an approximation to an even cat state at higher amplitudes. To achieve fidelities >0.99, we can only use $\beta \lesssim 0.5$. These results are shown in Fig. 6(b). It is interesting to note that when using the squeezed vacuum state as a resource, the fidelities for teleportation do not follow the general trends of the fidelity between the ideal and approximate resource, as is the case with using the squeezed single photon as a resource.
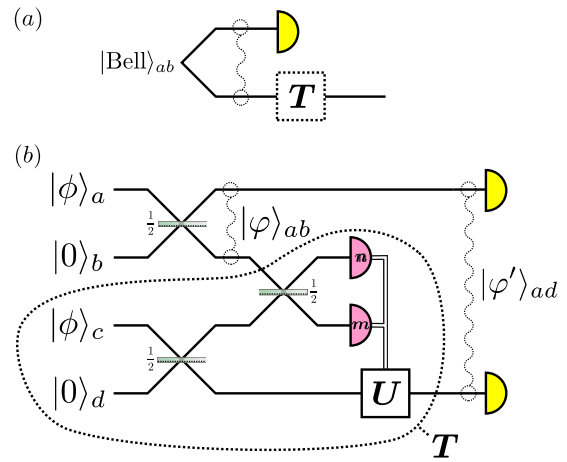

FIG. 7. (Color online) (a) By measuring mode a of a Bell state in an arbitrary basis, an arbitrary state can be prepared in mode b. This arbitrary state can be subsequently sent through a teleporter, T. (b) Replacing the teleporter T with the teleporter described in Fig. 1 and delaying the measurement of mode a, until *after* the teleportation, results in an entanglement swapping scheme analogous to (a), where the Bell state is created by sending the state $|\phi\rangle_a$ through a beam splitter and the teleporter consists of the circuit inside the dotted region. By teleporting one qubit in the Bell state before measuring the other qubit in that Bell state, we are effectively teleporting all possible states. The homodyne measurements on modes a and d can be performed at the end in the form of state tomography. The squiggly lines represent entanglement between qubits.

B. Entanglement swapping

To truly demonstrate a teleportation protocol, one would like to show that the protocol is capable of teleporting an unknown arbitrary state. We will show how this can be done by casting the teleportation of an arbitrary unknown state into an entanglement swapping scheme. Refer to the caption in Fig. 7 for details.

To characterize how well this protocol works, we will calculate the fidelity between the two-qubit entangled state in modes a and b, after the first beam splitter, and the two-qubit entangled state in modes a and d, after the photon number measurements of modes b and c. In our calculations, as with the teleportation scheme, we have omitted the even photon-number results. The average fidelity, over the odd photon-number results, is shown in Fig. 8. At first glance, it looks like the entanglement swapping protocol does not work as well as the teleportation scheme. This is because, for a given resource state of amplitude β, the input state to be teleported would have an amplitude α and the cat state approximations are much better at lower amplitudes. For the entanglement swapping scheme, we begin with two states of amplitude β, which means we are already starting with lower fidelity approximations. Nevertheless, for $\beta \lesssim 1.2$, the fidelity is always >0.99.

Using squeezed vacuum state to approximate an even cat state does not perform as well. To achieve fidelities of >0.99, we could only use $\beta \lesssim 0.45$.

VI. ERROR ANALYSIS

Until now, we have been treating the proposed experiments as lossless systems, however, propagation loss, imper-
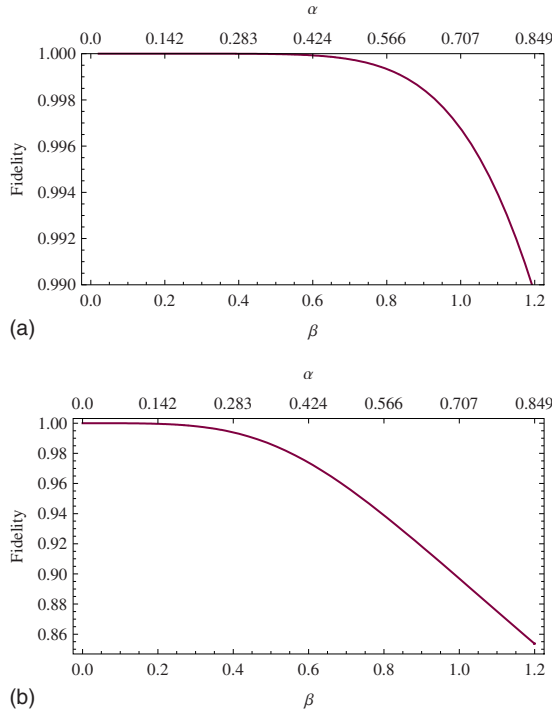
FIG. 8. (Color online) Fidelity for an entanglement swapping protocol using (a) $|\phi\rangle = \hat{S}_{r'}|1\rangle$ and (b) $|\phi\rangle = \hat{S}_{r''}|0\rangle$. Notice different scales for the fidelity.

fect detectors, and loss in the source are likely to be issues in the experiment. In this section, we will investigate the effects of loss in the proposed experiment.

Errors could occur in a number of places: the state to be teleported and the resource state could be made imperfectly; there could be photon loss at the optical elements; and of course, inefficient photon number and homodyne detection. In this paper, we will assume that imperfect creation of the state to be teleported and any inefficiencies in the homodyne detection of the output state reflect our inability to analyze how well the scheme worked and are not fundamental to the scheme itself. These errors can be compensated for in the postmeasurement analysis of the data. The calculations in this section were complicated by the additional loss modes, therefore, we needed to limit ourselves to smaller values of β. The photon-number expansion of the states in this section were truncated at $n=6$ for the teleportation scheme and $n =5$ for the entanglement swapping scheme which gave accurate results up to $\beta=1$ and $\beta=0.5$, respectively.

A. Teleportation

We will model the imperfect creation of the resource state by placing a beam splitter of transmittivity η_1 just after the source and the inefficient photodetection by placing beam splitters of transmittivity η_2 just before the detectors, as is shown in Fig. 9. We assume that both detectors will have the same inefficiencies. η ranges from 0 to 1 and at $\eta=1$, we have a lossless system. Our loss calculations have been carried out for the same scenario as in Sec. V, however, the loss in mode b will decrease the amplitude of the resource state
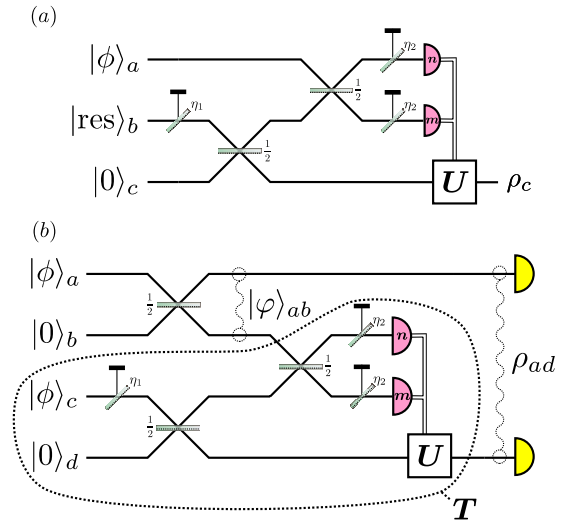

FIG. 9. (Color online) Teleportation scheme (a) and entanglement swapping scheme (b) with additional beam splitters of transmittivity: η_1 to model the imperfect creation of the resource state $|\text{res}\rangle_b = \hat{S}_r|1\rangle_b$, and η_2 to model the inefficiencies in the photodetectors. The input state is $|\phi\rangle_a = \hat{S}_{r'}|1\rangle_a$ where $r' = r_{\text{opt}}(\sqrt{\eta_1}\alpha)$ for the teleportation scheme and $r' = r_{\text{opt}}(\sqrt{\eta_1}\beta)$ for the entanglement swapping scheme to match the amplitude of the lossy resource state.

$|\text{res}\rangle_b = \hat{S}_r|1\rangle_b$ by $\sqrt{\eta_1}$. To match this, our states to be teleported will need to be $|\phi\rangle_a = |\sqrt{\eta_1}\alpha\rangle_a$, $\hat{S}_{r'}|1\rangle_a$, and $\hat{S}_{r''}|0\rangle_a$, where $r' = r_{\text{opt}}(\sqrt{\eta_1}\alpha)$ and $r'' = r_{\text{opt-v}}(\sqrt{\eta_1}\alpha)$. Figure 10 shows the fidelity as a function of η_1 and η_2 using $|\text{res}\rangle_b = \hat{S}_r|1\rangle_b$ and teleporting $|\phi\rangle_a = \hat{S}_{r'}|1\rangle_a$ (a) and $|\alpha\rangle_a$ (b) for $\beta=0.5$ (solid)
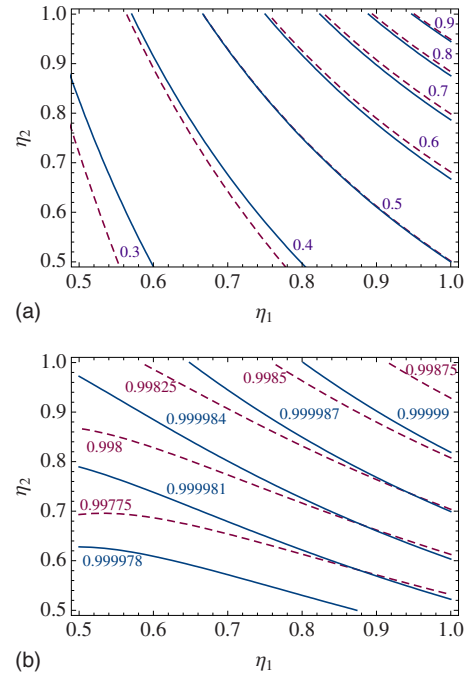

FIG. 10. (Color online) Contour plots of the fidelity for the teleportation scheme as a function of η_1 and η_2 for $\beta=0.5$ (solid) and $\beta=1.0$ (dashed): (a) $|\text{res}\rangle = \hat{S}_r|1\rangle$ and $|\phi\rangle = \hat{S}_{r'}|1\rangle$; (b) $|\text{res}\rangle = \hat{S}_r|1\rangle$ and $|\phi\rangle = |\alpha\rangle$.

and $\beta=1.0$ (dashed). As expected, loss has less effect on the fidelity at lower β, unfortunately, for $|\phi\rangle_a=\hat{S}_{r'}|1\rangle_a$, decreasing β does not improve the fidelity in the high-fidelity regime where one would like to perform experiments. Teleporting $|\phi\rangle_a=|\alpha\rangle_a$ is largely unaffected by loss. At both amplitudes, the fidelity remains extremely high.

To compare these fidelities with those for other states, we have taken a slice through the contour plots at $\eta_1=\eta_2$ and plotted the fidelity as a function of the equal losses. This is shown in Fig. 11. We have calculated the fidelity for teleporting a selection of ideal input states using both an ideal odd cat state and the squeezed single photon approximation as resources. Where possible, we have also teleported approximations to the ideal input states. This was done for $\beta=0.5$ and $\beta=1.0$. This gives an idea of how much of the effect of loss is inherent to the scheme and how much is a result of the approximate input and resource states. At $\beta=0.5$, it is difficult to distinguish between the results for any of these variations between ideal and approximate input and resource states. At this amplitude, the effects of loss are fundamental to the scheme itself. It is interesting to note that for $|\phi\rangle_a=\hat{S}_{r'}|1\rangle_a$ (or $|\phi\rangle_a=|\alpha\rangle_a-|-\alpha\rangle_a$), in the limit of $\eta_1\rightarrow0$, the input state amplitude is matched such that $\alpha\rightarrow0$, in which case, the input state becomes $|\phi\rangle_a\rightarrow|1\rangle_a$ and the output state will be $|\phi'\rangle_c=|0\rangle_c$ resulting in a fidelity which goes to 0. However, for any other input state, as $\eta_1\rightarrow0$, the input state will tend to $|\phi\rangle_a\rightarrow|0\rangle_a$. The output state will still be $|\phi'\rangle_c=|0\rangle_c$ resulting in a fidelity which goes to 1. This is why the loss seems to have a greater effect on the fidelity for teleporting $|\phi\rangle_a=\hat{S}_{r'}|1\rangle_a$, and $|\phi\rangle_a=|\alpha\rangle_a-|-\alpha\rangle_a$ than any other state.

Increasing the amplitude to $\beta=1.0$ does not have much effect on teleporting the odd cat state (and its approximations), but it does decrease the fidelity for the other states. In attempting high-fidelity experiments, low loss levels will be essential when teleporting states similar to $|\phi\rangle_a=\hat{S}_{r'}|1\rangle_a$ and $|\phi\rangle_a=|\alpha\rangle_a-|-\alpha\rangle_a$. States closer to $|\phi\rangle_a=|\alpha\rangle_a+|-\alpha\rangle_a$, $|\phi\rangle_a=|\alpha\rangle_a$, and their approximations are more forgiving.

B. Entanglement swapping

In the entanglement swapping protocol, we treat modes a and b as the input state to the teleporter and ignore loss in these modes in the analysis of the effects of loss on the teleporter, which has been modeled in much the same way as in Sec. VI A. We were only able to get reliable fidelities for $\beta=0.5$ as higher values of β would require higher truncation of the photon number which, for a seven-mode calculation, was not computationally tractable. These fidelities are shown in Fig. 12.

At this amplitude, we can see that there is not much difference between performing the entanglement swapping with an ideal odd cat state or the squeezed single photon. Both are quite severely affected by loss. The ideal even cat is much more tolerant to loss whereas the squeezed vacuum is less so, however, still better than the odd cat and squeezed single photon.

VII. DISCUSSION

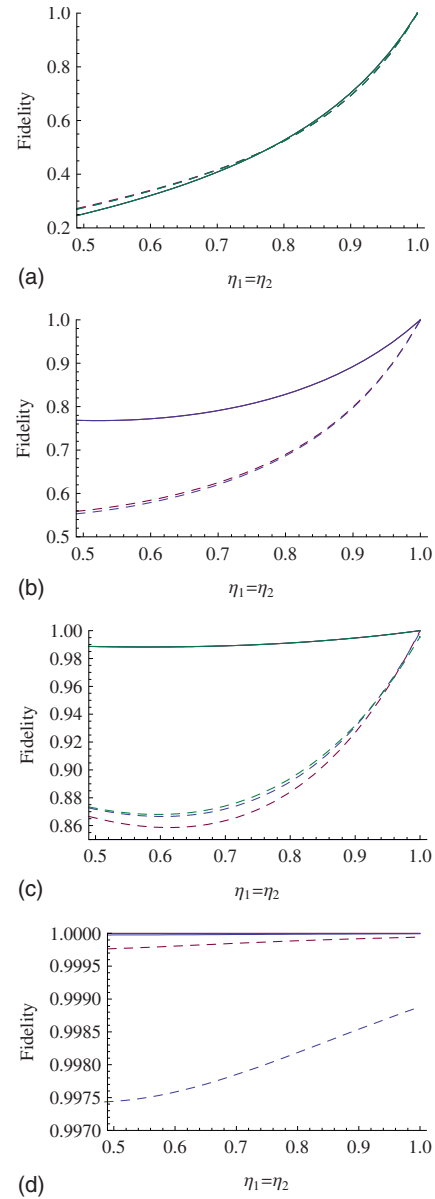The squeezed single photon turns out to be a great resource for high-fidelity teleportation of small-amplitude co-

FIG. 11. (Color online) The fidelity for the teleportation scheme as a function of η_1 and η_2, where $\eta_1=\eta_2$ for $\beta=0.5$ (solid) and $\beta=1.0$ (dashed). (a) $|\text{res}\rangle=|\beta\rangle-|-\beta\rangle$ and $|\phi\rangle=|\alpha\rangle-|-\alpha\rangle$ (red), $|\text{res}\rangle=\hat{S}_r|1\rangle$ and $|\phi\rangle=|\alpha\rangle-|-\alpha\rangle$ (blue), and $|\text{res}\rangle=\hat{S}_r|1\rangle$ and $|\phi\rangle=\hat{S}_{r'}|1\rangle$ (green). The fidelities for these states are so similar, they are practically indistinguishable. (b) From top to bottom, $|\text{res}\rangle=|\beta\rangle-|-\beta\rangle$ and $|\phi\rangle=\frac{1}{2}|\alpha\rangle-\frac{\sqrt{3}}{2}|-\alpha\rangle$ (red), and $|\text{res}\rangle=\hat{S}_r|1\rangle$ and $|\phi\rangle=\frac{1}{2}|\alpha\rangle-\frac{\sqrt{3}}{2}|-\alpha\rangle$ (blue). For $\alpha=0.5$, the fidelities are also practically indistinguishable. (c) From top to bottom, $|\text{res}\rangle=\hat{S}_r|1\rangle$ and $|\phi\rangle=\hat{S}_r|0\rangle$ (green), $|\text{res}\rangle=\hat{S}_r|1\rangle$ and $|\phi\rangle=|\alpha\rangle+|-\alpha\rangle$ (blue), and $|\text{res}\rangle=|\beta\rangle-|-\beta\rangle$ and $|\phi\rangle=|\alpha\rangle+|-\alpha\rangle$ (red). Again, practically indistinguishable at $\alpha=0.5$. (d) From top to bottom, $|\text{res}\rangle=|\beta\rangle-|-\beta\rangle$ and $|\phi\rangle=|\alpha\rangle$ (red), and $|\text{res}\rangle=\hat{S}_r|1\rangle$ and $|\phi\rangle=|\alpha\rangle$ (blue). Notice different scales for the fidelity.

herent state superpositions. Due to its property of always containing at least one photon, the teleportation scheme will always succeed with a probability greater than 50%. We have shown that the squeezed single photon can be used to tele-
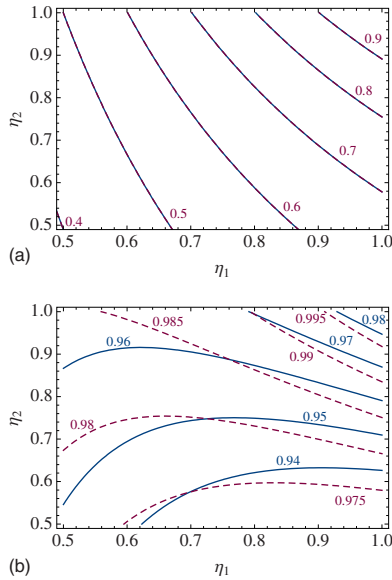
FIG. 12. (Color online) Contour plots of the fidelity for the entanglement swapping scheme as a function of η_1 and η_2 for $\beta = 0.5$ where (a) $|\phi\rangle = |\alpha\rangle - |-\alpha\rangle$ (dashed) and $|\phi\rangle = \hat{S}_{r'}|1\rangle$ (solid), and (b) $|\phi\rangle = |\alpha\rangle + |-\alpha\rangle$ (dashed) and $|\phi\rangle = \hat{S}_{r'}|0\rangle$ (solid).

port a coherent state, a squeezed single photon, and a squeezed vacuum, which despite not being a very good resource for teleportation itself, is a good approximation to an

even cat state at very small amplitudes. In-principle teleportation of arbitrary coherent state superpositions can be demonstrated using the squeezed single photons as inputs to an entanglement swapping protocol. This also works with high fidelity at small amplitudes. Teleportation is the implementation of the identity gate and these results suggest that demonstration of more complicated nontrivial gates will be practical in the foreseeable future.

Our analysis of the effects of imperfect source preparation and inefficient detection has shown this setup to be very fragile in this regard. It would be possible to do high-fidelity teleportation of states like the coherent state and the even cat state with a lossy system, but states which are more similar to the odd cat state degrade very quickly, even with low loss. It looks like this fragility is a property of the gate, and not just the approximation of the states, however, at higher amplitudes, the fidelity is further affected by loss when using the approximate states.

In this paper we have analyzed coherent state teleportation using small-amplitude approximations to cat states, however, there has been progress in creating larger amplitude cat state approximations via cat state amplification [10,20] and ancilla-assisted photon subtraction [21].

[1] T. C. Ralph, A. Gilchrist, G. J. Milburn, W. J. Munro, and S. Glancy, Phys. Rev. A **68**, 042319 (2003).

[2] A. P. Lund, T. C. Ralph, and H. L. Haselgrove, Phys. Rev. Lett. **100**, 030503 (2008).

[3] E. Knill, R. Laflamme, and G. J. Milburn, Nature (London) **409**, 46 (2001).

[4] P. Kok, W. J. Munro, K. Nemoto, T. C. Ralph, J. P. Dowling, and G. J. Milburn, Rev. Mod. Phys. **79**, 135 (2007).

[5] D. Gottesman and I. L. Chuang, Nature (London) **402**, 390 (1999).

[6] S. J. van Enk and O. Hirota, Phys. Rev. A **64**, 022313 (2001).

[7] H. Jeong, M. S. Kim, and J. Lee, Phys. Rev. A **64**, 052308 (2001).

[8] D. Bouwmeester, J. W. Pan, K. Mattle, M. Eibl, H. Weinfurter, and A. Zeilinger, Nature (London) **390**, 575 (1997).

[9] A. P. Lund and T. C. Ralph, Phys. Rev. A **71**, 032305 (2005).

[10] A. P. Lund, H. Jeong, T. C. Ralph, and M. S. Kim, Phys. Rev. A **70**, 020101(R) (2004).

[11] A. Ourjoumtsev, R. Tualle-Brouri, J. Laurat, and P. Grangier, Science **312**, 83 (2006).

[12] J. S. Neergaard-Nielsen, B. M. Nielsen, C. Hettich, K.

Molmer, and E. S. Polzik, Phys. Rev. Lett. **97**, 083604 (2006).

[13] A. Ourjoumtsev, H. Jeong, R. Tualle-Brouri, and P. Grangier, Nature (London) **448**, 784 (2007).

[14] C. H. Bennett, G. Brassard, C. Crépeau, R. Jozsa, A. Peres, and W. K. Wootters, Phys. Rev. Lett. **70**, 1895 (1993).

[15] H. Jeong and T. C. Ralph, *Quantum Information with Continuous Variables of Atoms and Light* (Imperial College, London, 2007), Vol. 1, Chap. 9, pp. 159–177.

[16] M. A. Nielsen, e-print arXiv:quant-ph/0504097v2, Rev. Math. Phys. (to be published).

[17] D. F. Walls and G. J. Milburn, *Quantum Optics* (Springer, New York, 1984).

[18] M. Dakna, T. Anhut, T. Opatrný, L. Knoll, and D.-G. Welsch, Phys. Rev. A **55**, 3184 (1997).

[19] A. E. B. Nielsen and K. Mølmer, Phys. Rev. A **76**, 043840 (2007).

[20] H. Jeong, A. P. Lund, and T. C. Ralph, Phys. Rev. A **72**, 013801 (2005).

[21] H. Takahashi, K. Wakui, S. Suzuki, M. Takeoka, K. Hayasaka, A. Furusawa, and M. Sasaki, e-print arXiv:0806.2965v1.